Comparison between CASPT2 and DFT in the Study of $Ni(C_2H_4)_2$ Complexes

Fernando Bernardi,* Andrea Bottoni,* Michele Calcinari, and Ivan Rossi

Dipartimento di Chimica "G. Ciamician", Universita' di Bologna, via Selmi 2, 40126 Bologna, Italy

Michael A. Robb

Department of Chemistry, King's College London, Strand, London WC2R 2LS, U.K.

Received: March 19, 1997[⊗]

In this paper we report the results of a comparative theoretical study at the CASSCF/CASPT2 and DFT levels of the potential energy surface associated with bis(ethylene)−nickel complexes. The computations predict the existence on the potential surface of only one minimum of D_{2d} symmetry: the other critical points located on the surface (corresponding to structures of C_{2v} and D_{2h} symmetries) are saddle points of higher order. The results have pointed out that (i) the inclusion of dynamic correlation does not change the topology of the surface; (ii) the DFT approach provides for these systems results very similar to those obtained at the CASSCF/CASPT2 level; (iii) an effective core potential (ECP) basis (LANL2DZ) can provide a reliable description for these metal−olefin clusters. The second and third points are of particular interest since they indicate that it is possible to use a cheap approach (DFT with an ECP basis) to investigate larger nickel−olefin clusters with bulky ligands on the metal atom, as those involved in catalyzed cycloaddition reactions.

Introduction

Methods based on density functional theory (DFT)[1] represent a versatile computational approach capable of describing successfully many problems previously covered exclusively by ab-initio HF and post-HF methods. The studies carried out during the last decade have shown that DFT-based methods, especially in the forms containing nonlocal corrections, provide geometries and energetics that are in better agreement with the experiment than the HF results (in particular for transition-metal complexes).[2] Furthermore, because of their computational expedience, these methods seem to be particularly suitable for describing large-size molecular systems containing metals. Since these methods are becoming more and more popular, it is nowadays particularly important to carry out a calibration of DFT methods for identifying strengths and weaknesses of the various functionals. To this purpose in the present paper we investigate the potential energy surface associated with the bis(ethylene)−nickel complex $Ni(C_2H_4)_2$. These clusters are a very interesting example of transition metal−olefin complexes. They provide very simple models for understanding the nature of the metal−olefin bond and also for studying catalyzed processes since complexes of this type, with additional ligands on the nickel atom, seem to be involved in homogeneously catalyzed [2+2] cycloaddition reactions.[3]

The existence of these chemical species has been proved by many studies carried out in the last two decades.[4] Using matrix isolation techniques, nickel atom has been demonstrated to react with ethylene when trapped in cryogenic conditions. Ozin et al.,[4a,b] using IR and UV−visible absorption spectroscopies, have shown the existence of three binary complexes $Ni(C_2H_4)_n$ (n = 1, 2, 3). More recently, the stoichiometry of these complexes has been definitely determined by examining the metal−ligand stretching vibrations in IR and Raman spectra.[4c] In two very recent studies,[4d,e] Mitchell et al., have demonstrated that 1:1 Ni−ethylene complexes can be synthesized at room temperature by producing nickel atoms from pulsed laser-induced multiphoton dissociation (MPD) of nickelocene.

While 1:1 ethylene-nickel complexes have been the subject of several theoretical investigations,[5a−e,g−l] only a few computations have been performed on bis(ethylene)−nickel clusters. The bonding in $Ni(C_2H_4)_2$ has been described by Siegbahn and Brandemark at the CASSCF level with the addition of contracted CI calculations.[5f] These authors have analyzed three different geometries of D_{2d}, D_{2h}, and C_{2v} symmetry, respectively. However, the topology of the potential energy surface remains in question since full geometry optimization has not been used and the nature of the various critical points has not been determined.

To performe our comparative analysis, we use different forms of nonlocal DFT methods to investigate the potential surface associated with the $Ni(C_2H_4)_2$ complex, and we compare these results to those obtained with the CASSCF method with large basis sets followed by a perturbation treatment up to second-order (CASPT2) to evaluate the dynamical correlation contribution.

Computational Methods

The CASSCF and CASPT2 computations reported in the paper have been carried out using the MOLCAS-3[6] program. The atomic natural orbital (ANO) basis[7a] suggested by Bauschlicher et al.,[7b] was used for the nickel atom, while the carbon and hydrogen atoms were described by the Dunning cc-pVDZ basis set.[8] This basis[9] is formed by a (Ni: 20s, 15p, 10d, 6f), (C: 7s, 6p, 4d, 2f), (H: 4s, 1p) primitive set contracted to [Ni: 7s, 6p, 4d, 2f], [C: 3s, 2p, 1d], [H2s, 1p].

The geometries of the various structures have been optimized at the CASSCF level with the gradient procedure. Single-point computations at the CASSCF-optimized geometries have been performed using the multireference perturbation approach suggested by Andersson et al. (CASPT2)[10] to include the dynamical correlation energy effects.

The active space used in the CASSCF geometry optimizations includes all the orbitals required to allow the proper description of the Ni−C forming bonds and to describe the low-lying states of the metal atom. Thus we have considered the π and π^* orbitals of the two ethylene moieties and the 4s and 3d orbitals

[⊗] Abstract published in *Advance ACS Abstracts,* August 1, 1997.

S1089-5639(97)00998-5 CCC: $14.00

of the nickel atom. These active orbitals form a space of 14 electrons in 10 orbitals. The size of the active space has been increased in the single-point CASPT2 computations. In this case, as suggested by Pierloot, Persson, and Roos,[5l] for each doubly occupied 3d orbital not taking part in the bond, we have added a correlating 4d orbital. The inclusion of these additional orbitals leads to an active space of 14 electrons in 12 orbitals for the D_{2d}, C_{2v}(planar), and C_{2v}(bent) structures and 14 electrons in 13 orbitals for the D_{2h} structure. With this active space the perturbation contributions are all smaller than 1.0 kcal/mol.

All the DFT computations have been performed with the Gaussian 92/DFT[11] series of programs using a local spin density (LSD)-optimized basis set of double-ζ quality in the valence shell plus polarization functions (DZVP).[12] Additional computations have been carried out with the effective core potential (ECP) LANL2DZ[13] basis set. In all cases, the geometries of the various critical points have been fully optimized with the gradient method and the nature of each critical point has been characterized by computing the harmonic vibrational frequencies. We have used a hybrid functional and two pure functionals, which are all implemented in Gaussian 92/DFT. The two pure functionals, denoted as BLYP and BP86, differ only in the correlation term and can be written as follows

$$E(\mathrm{S})_x + E(\mathrm{B88})_x + E_c$$

where $E(\mathrm{S})_x$ is the Slater exchange,[14a,b] $E(\mathrm{B88})_x$ is the Becke's 1988 nonlocal exchange functional corrections,[14c] and E_c is the correlation contribution including nonlocal corrections. In the BLYP functional E_c is the correlation functional of Lee, Yang, and Parr (LYP)[14d,e] including both local and nonlocal terms while in the BP86 functional E_c includes both the local functional of Perdew[14f] and his gradient corrections.[14g] The hybrid functional corresponds to Becke's three-parameter exchange functional[14i] as implemented in Gaussian 92/DFT and is denoted here as B3LYP.

Results and Discussion

A. CASSCF/CASPT2 Results. In this section we discuss the singlet potential energy surface obtained at the CASSCF and CASPT2 levels for the bis(ethylene)−Ni complex. This surface originates from the interaction of the $Ni(C_2H_4)$ complex in the singlet ground state with a second ethylene molecule. Four critical points, two with symmetry C_{2v}(bent and planar) and two with symmetry D_{2h} and D_{2d} have been located. The corresponding structures are shown in Figure 1, while the corresponding energies and the optimum values of the geometrical parameters are reported in Table 1. While the existence of the C_{2v}(planar) structure has never been pointed out, those of the C_{2v}(bent), D_{2h}, and D_{2d} structures have been already documented by Siegbahn and Brandemark.[5f] However these structures were not completely optimized, and the nature of the critical points was not determined.

The structure with D_{2d} symmetry, where the two planes that contain the C−C bonds of the two olefins and the metal atom form a dihedral angle ω of 90° (see Figure 1a), has the lowest CASSCF energy. The formation of the complex, which is characterized by a Ni−C bond length of 2.021 Å, causes significant changes in the ethylene structure. The C−C bond becomes significantly longer (1.399 Å) than that in ethylene (1.332 Å) and a nonnegligible rehybridization of the carbon atoms takes place: the two methylene hydrogen atoms are bent 18.8° out of the ethylene molecular plane (see the out of plane angle ϵ formed by the bisector of the HCH angle and the C−C direction). The C_{2v}(planar) structure is only a few kcal/mol above the D_{2d} form (6.89 kcal/mol). In this structure, the Ni atom and the four carbon atoms lie in the same plane but the two ethylene C−C bonds are not parallel. In the C_{2v}(bent) form, the two C−C bonds become parallel but the Ni atom is not in the plane of the four carbon atoms. This point of the potential surface has a CASSCF energy that is 18.05 kcal/mol higher than that of D_{2d}. The lengths of the C−C and Ni−C bonds of the two C_{2v} complexes are very close to the values found for the D_{2d} structure. Also the pyramidalization angle ϵ does not

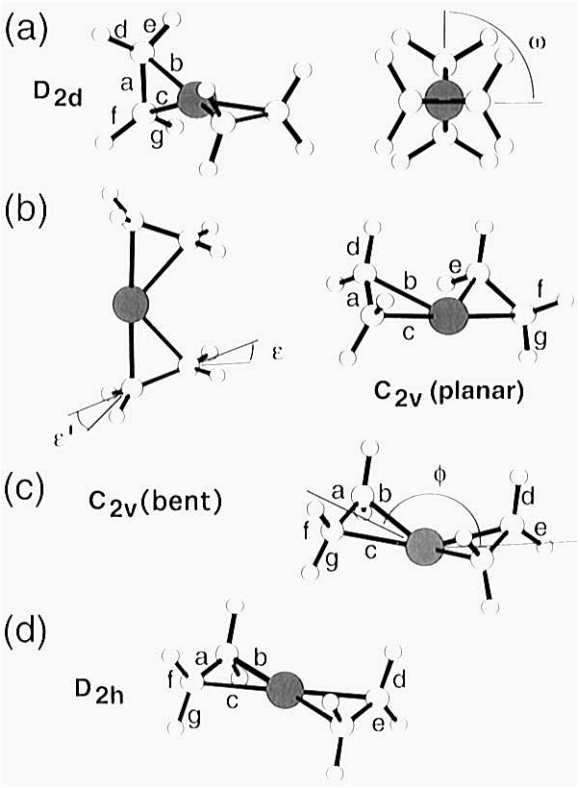

Figure 1. Schematic geometries of the D_{2d} (a), C_{2v}(planar) (b), C_{2v}(bent) (c), and D_{2h} (d) structures of $Ni(C_2H_4)_2$ computed at the CASSCF and DFT levels of theory.

TABLE 1: Optimum Geometries[a] and Relative Energies $E^{b,c}$ for the D_{2d}, C_{2v}(Planar), C_{2v}(Bent) and D_{2h} Structures of the $Ni(C_2H_4)_2$ Complex Obtained at the CASSCF Level of Theory Using the ANO Basis for Nickel and the cc-pVDZ Basis for Carbon and Hydrogen

	D_{2d}	C_{2v}(planar)	C_{2v}(bent)	D_{2h}
a	1.399 [1.408]	1.397	1.397 [1.376]	1.373 [1.376]
b	2.021 [2.070]	2.022	2.055 [2.312]	2.121 [2.312]
c	2.021 [2.070]	2.015	2.055 [2.312]	2.121 [2.312]
d	1.085	1.084	1.083	1.083
e	1.085	1.084	1.087	1.083
f	1.085	1.084	1.083	1.083
g	1.085	1.084	1.087	1.083
∠*ab*	69.8	69.5	70.2	71.1
∠*ac*	69.8	70.1	70.2	71.1
∠*de*	115.0	115.0	115.2	116.4
∠*fg*	115.0	115.5	115.2	116.4
ϕ		180.0	148.5 [103.0]	180.
ω	90.0	0.0	0.0	0.0
ϵ	18.8	18.5	18.7	11.6
ϵ'	18.8	20.2	18.7	11.6
E	0.00	6.89	18.05	36.56
$E^{(2)}$	0.00	5.07	17.31	18.96

[a] Bond lengths are in angstroms and angles in degrees. [b] Kcal/mol. [c] The absolute CASSCF and CASPT2 energies of the D_{2d} structure are −1663.014 54 and −1664.273 75 hartree, respectively. [d] $E^{(2)}$ represents the CASPT2 energy obtained at the CASSCF-optimized geometries (values in brackets are taken from ref 5f; see Figure 1 for the notations of the calculated geometric parameters).

change significantly, being 18.5° (ϵ) and 20.2° (ϵ') in C_{2v} (planar) and 18.7° in C_{2v} (bent).

The highest in energy structure (36.59 kcal/mol above D_{2d}) has a D_{2h} symmetry (nickel and carbon atoms are in the same plane, and the two C−C bonds are parallel). In this case the Ni−C bond is longer (2.121 Å) than in the previous structures with a consequent stronger double-bond character of the ethylene C−C bonds (1.373 Å) and a less pronounced rehybridization of the carbon atoms ($\epsilon = 11.6°$).

For the D_{2d} and the D_{2h} forms, the geometrical parameters compare quite well with those computed by Brandemark and Siegbahn (see values in brackets reported in Table 1). However, for the C_{2v}(bent) structure our results are characterized by a longer C−C bond (more single-bond character) and a shorter Ni−C bond. Furthermore in this structure, the angle ϕ is much larger (148.5°) than the value obtained by Siegbahn (103°) (ϕ is the dihedral angle between the two planes that contain the nickel atom and the two double bonds). These differences probably arise from the fact that the geometries of Brandemark and Siegbahn were not fully optimized with the gradient method.

The inclusion of the dynamical correlation contributions (CASPT2 computations) does not change the energetic order of the four critical points (the D_{2d} form remains the lowest energy structure) but affects the various energy gaps. While the energy differences $D_{2d}-C_{2v}$(planar) and $D_{2d}-C_{2v}$(bent) only slightly decrease (they become 5.07 and 17.31 kcal/mol respectively), the difference $D_{2d}-D_{2h}$ strongly decreases (from 36.56 to 18.96 kcal/mol). These results suggest that the topology of the surface does not change after inclusion of correlation energy.

B. DFT Results. The results obtained at this level of theory are collected in Table 2. From this table it is evident that the three functionals provide almost identical geometries, which are very similar to those found at the CASSCF level. This suggests that for these systems the inclusion of the correlation contribution does not affect critically the geometry. The only exception is represented by the C_{2v}(bent) structure: in this case the ϕ angle becomes 159.2° and 158.0° at the BLYP/DZVP and BP86/DZVP levels, respectively, and increases further when the B3LYP functional is used (170.1°).

The most interesting result is that, at the DFT level, the energetic order of the four critical points is identical to that found at the CASPT2 level and the energy differences are very similar. The D_{2d} critical point corresponds again to the most stable structure with the C_{2v}(planar) structure only a few kcal/mol higher in energy. This difference is 5.04, 5.64, and 5.03 kcal/mol with the B3LYP, BLYP, and BP86 functionals, respectively. Also the $D_{2d}-C_{2v}$(bent) and the $D_{2d}-D_{2h}$ differences compare very well with the CASPT2 results. These quantities are 12.80 and 12.84 kcal/mol, respectively, at the B3LYP/DZVP level, are 13.24 and 14.53 kcal/mol at the BLYP/DZVP level, and become 14.09 and 15.94 kcal/mol with the BP86 functional. From these values it is also evident that the difference between the C_{2v}(bent) and the D_{2h} structures becomes almost negligible with the B3LYP functional in agreement with the large increase of the ϕ angle. All these results suggest that the topology of the surface does not change at the DFT level and that we can characterize the nature of the various critical points by performing full Hessian computations at this level of theory. A comparison between the results obtained with the three functionals also indicates that the BP86 functional provides the best agreement with the CASPT2 data.

The computation of the Hessians has pointed out that the D_{2d} structure is the only real minimum of the surface (all real frequencies), while the remaining critical points are saddle points of index 1 (C_{2v}(planar), one imaginary frequency), index 2 (C_{2v}(bent), two imaginary frequencies), and index 3 (D_{2h}, three imaginary frequencies). Figure 2 illustrates for each saddle point the directions in which the atoms move in the normal coordinates corresponding to the imaginary frequencies. For the C_{2v}(planar) structure (Figure 2a), this motion corresponds to a rotation leading the two NiCC planes from a coplanar arrangement to an orthogonal arrangement; thus, the C_{2v}(planar) critical point is a transition state connecting two equivalent D_{2d} structures. For the C_{2v}(bent), the larger imaginary frequency (231.9i) is still a rotation of the two NiCC planes, while the smaller frequency (199.1i) corresponds to a motion leading to the C_{2v}(planar) structure. In the case of the D_{2h} structure, two imaginary frequencies correspond to the two motions previously described, while the third imaginary frequency (306.6i) is an out-of-plane bending of the four carbon atoms and connects this point to the C_{2v}(bent) point.

Since olefin−nickel complexes involved in homogeneous catalysis are much larger than the system investigated here (they usually involve additional cumbersome ligands on the metal), it becomes quite important to demonstrate not only that all-electron DFT-based methods are suitable to describe this type of molecular systems but also that it is possible to provide a reliable description using less expensive basis sets. Effective core potential (ECP) approaches are particularly interesting and promising from this point of view since they can deal cheaply

TABLE 2: Optimum Geometries[a] and Relative Energies $E^{b,c}$ for the D_{2d}, C_{2v}(Planar), C_{2v}(Bent) and D_{2h} Structures of the $Ni(C_2H_4)_2$ Complex Obtained with the DFT Method (B3LYP, BLYP, and BP86 Functionals) and the DZVP Basis Set[d]

	B3LYP	BLYP	BP86	B3LYP	BLYP	BP86
		D_{2d}			C_{2v}(planar)	
a	1.396	1.408	1.406	1.396	1.409	1.408
b	1.990	2.013	1.986	2.009	2.029	1.996
c	1.990	2.013	1.986	1.976	1.998	1.972
d	1.090	1.097	1.099	1.090	1.097	1.099
e	1.090	1.097	1.099	1.090	1.097	1.099
f	1.090	1.097	1.099	1.091	1.099	1.100
g	1.090	1.097	1.099	1.091	1.099	1.100
∠*ab*	69.5	69.5	69.3	68.2	68.3	68.3
∠*ac*	69.5	69.5	69.3	70.7	70.7	70.1
∠*de*	115.4	115.5	115.5	115.3	115.4	115.3
∠*fg*	115.4	115.5	115.5	115.8	115.9	115.9
ϕ				180.0	180.0	180.0
ω	90.0	90.0	90.0	0.00	0.0	0.0
ϵ	15.5	15.2	15.2	15.5	15.4	16.2
ϵ'	15.5	15.2	15.2	17.8	17.9	18.3
E	0.00	0.00	0.00	5.04	5.64	5.03
		C_{2v}(bent)			D_{2h}	
a	1.381	1.398	1.397	1.379	1.392	1.390
b	2.047	2.053	2.022	2.050	2.068	2.038
c	2.047	2.053	2.022	2.050	2.068	2.038
d	1.089	1.096	1.098	1.090	1.097	1.099
e	1.090	1.098	1.101	1.090	1.097	1.099
f	1.089	1.096	1.098	1.090	1.097	1.099
g	1.090	1.098	1.101	1.090	1.097	1.099
∠*ab*	70.3	70.1	69.8	70.4	70.3	70.1
∠*ac*	70.3	70.1	69.8	70.4	70.3	70.1
∠*de*	116.3	116.0	116.0	116.4	116.4	116.5
∠*fg*	116.3	116.0	116.0	116.4	116.4	116.5
ϕ	170.1	159.2	158.0	180.0	180.0	180.0
ω	0.00	0.0	0.0	0.00	0.0	0.0
ϵ	11.7	13.1	13.4	11.6	11.3	11.5
ϵ'	11.7	13.1	13.4	11.6	11.3	11.5
E	12.80	13.24	14.09	12.84	14.53	15.94

[a] Bond lengths are in angstroms and angles in degrees. [b] Kcal/mol. [c] The absolute B3LYP, BLYP, and BP86 energies of the D_{2d} structure are −1665.310 91, −1665.299 31, and −1665.540 82, hartree, respectively. [d] See Figure 1 for the notations of the calculated geometric parameters.

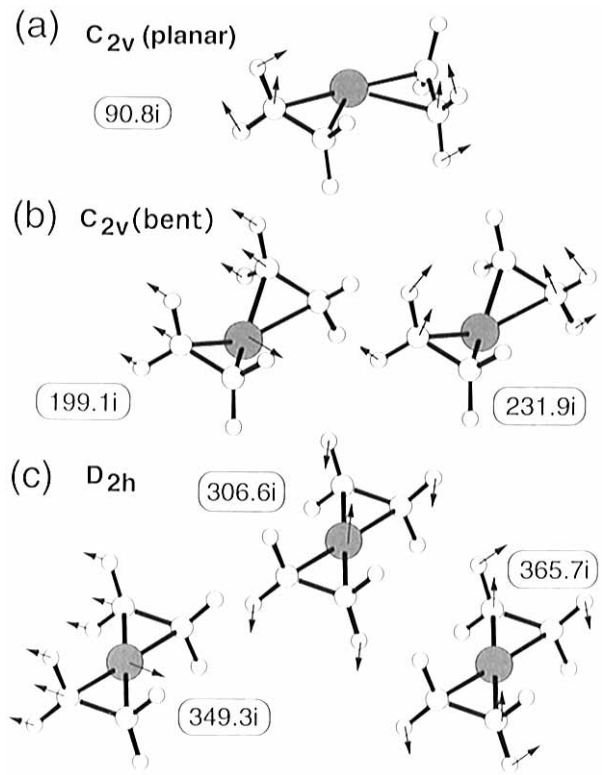

Figure 2. Representation of the imaginary normal coordinates (arrows illustrate the directions of atom displacements) computed at the DFT level with the DZVP basis set and the BP86 functional. Imaginary frequencies are given in cm^{-1}.

TABLE 3: Optimum Geometries[a] and Relative Energies *E*[b] for the D_{2d}, C_{2v}(Planar), C_{2v}(Bent), and D_{2h} Structures of the $Ni(C_2H_4)_2$ Complex Obtained with the DFT Method (BP86 Functional) and the LANL2DZ Basis Set

	D_{2d}	C_{2v}(planar)	C_{2v}(bent)	D_{2h}
a	1.419	1.421	1.411	1.404
b	2.021	2.034	2.056	2.070
c	2.021	2.001	2.056	2.070
d	1.099	1.098	1.097	1.099
e	1.099	1.098	1.101	1.099
f	1.099	1.100	1.097	1.099
g	1.099	1.100	1.101	1.099
∠*ab*	69.4	68.1	69.9	70.2
∠*ac*	69.4	70.6	69.9	70.2
∠*de*	115.6	115.5	116.1	116.5
∠*fg*	115.6	116.0	116.1	116.5
ϕ		180.0	156.2	180.
ω	90.0	0.0	0.0	0.0
ϵ	15.8	15.7	13.9	13.0
ϵ'	15.8	18.5	13.9	13.0
E	0.00	4.82	13.38	15.90

[a] Bond lengths are in angstroms and angles in degrees. [b] The energy of the D_{2d} structure is −326.609 88 hartree.

with molecular systems involving transition metals and larger ligands. Thus their calibration becomes particularly important.

To elucidate this point we have reinvestigated the potential energy surface using the ECP variant with LANL2DZ basis and the BP86 functional. The results are reported in Table 3 and are almost identical to those obtained with the all-electron basis DZVP. The energy order of the four critical points obtained at this level of accuracy remains the same, and only negligible variations of the energy differences with respect to the BP86/DZVP results have been found: the energy difference between the C_{2v}(planar) and the D_{2d} structure changes from 5.03 to 4.82 kcal/mol, while the $D_{2d}-C_{2v}$(bent) and the $D_{2d}-D_{2h}$ differences change from 14.09 to 13.38 kcal/mol and from 15.94 to 15.90 kcal/mol respectively.

TABLE 4: Bond Energies BE[a] for the $Ni(C_2H_4)_2$ Complex[b] Obtained at Various Computational Levels

	CASSCF[c]	CASPT2[c]	B3LYP[d]	BLYP[d]	BP86[d]
BE	59.7	48.1	38.9	40.2	45.8 (42.6)

[a] kcal/mol. [b] The optimum geometrical parameters (angstroms and degrees) for the system at the asymptotic limit ($Ni(C_2H_4) + C_2H_4$) are as follows: CASSCF, $a = 1.426$, b, c = 1.990, d, e, f, g = 1.086, $\epsilon = 157.0$, r(C═C) = 1.341; B3LYP, $a = 1.434$, b, c = 1.892, d, e, f, g = 1.093, $\epsilon = 157.2$, r(C═C) = 1.337; BLYP, $a = 1.445$, b, c = 1.912, d, e, f, g = 1.100, $\epsilon = 157.9$, r(C═C) = 1.347; BP86, $a = 1.442$ (1.458), b, c = 1.890 (1.917), d, e, f, g = 1.102 (1.102), $\epsilon = 157.7$ (157.0), r(C═C) = 1.345 (1.321). [c] Values obtained with the ANO basis set. [d] Values obtained with the DZVP basis set and the LANL2DZ basis set (in parentheses).

A further interesting point that is worth to discuss is given by the bond energy values of the $Ni(C_2H_4)_2$ complex computed at the various computational levels. These values, which are reported in Table 4, correspond to the energy difference between the asymptotic limit (represented by the $Ni(C_2H_4)$ complex and a non interacting ethylene molecule) and the D_{2d} complex, which forms without any barrier and is lower in energy than the reactants. Also in this case the BP86 functional provides the best result: the binding energy value computed at this level is 45.8 kcal/mol, which is in good agreement with the value of 48.1 kcal/mol obtained at the CASPT2 level. This value slightly decreases when the effective basis set LANL2DZ is used and becomes 42.6 kcal/mol.

Conclusions

In this paper we have investigated the potential energy surface for the $Ni(C_2H_4)_2$ complexes using a CASSCF/CASPT2 approach and a DFT approach. At both levels of theory we have found that four critical points exist on the potential surface. On the basis of the symmetry of the corresponding molecular structures, these points have been denoted as D_{2d}, C_{2v}(planar), C_{2v}(bent), and D_{2h}. The D_{2d} critical point corresponds to the lowest energy structure and represents the only minimum of the surface as demonstrated by the frequency computations performed at the DFT level. This structure should correspond to the real intermediate experimentally observed by Ozin et al.[4a,b] The three additional critical points C_{2v}(planar), C_{2v}(bent), and D_{2h} correspond to saddle-points of index 1, 2, and 3, respectively.

These computations have pointed out that the agreement between the CASSCF/CASPT2 and DFT results is very good since the geometries obtained at the two levels are very similar, the energetic order of the four structures is the same, and the binding energy is satisfactorily reproduced. In particular the BP86 functional seems to provide the best results. The good performance of this functional is even more confirmed by the comparison between the calculated vibrational frequencies and the experimental ones: for example, the experimental values of the relevant γ_{CC} and δ_{CH2} vibrational modes are 1223 and 1465 cm^{-1}, respectively[4a,b] which compare very well with the theoretical values (BP86/DZVP level) of 1234 and 1508 cm^{-1}. Therefore it follows that we can use with confidence a cheaper DFT approach for studying this type of metal−olefin systems. This approach has two advantages: firstly, it allows one to perform reliable computations on metal−olefin complexes with large ligands; secondly, it allows one to include directly the effects of dynamical correlation on geometry and frequency computations.

Another important comment concerns the results obtained with the ECP basis set LANL2DZ. We have shown that this basis is capable of reproducing quite accurately the data provided by more accurate all-electron basis sets. These results are particularly important and promising since the validation of a computational treatment based on DFT theory and ECP basis sets extends the possibility of a theoretical investigation to more realistic olefin−metal complexes as those involved in catalyzed cycloaddition.

References and Notes

(1) Parr, R. G.; Yang,W. *Density-Functional Theory of Atoms and Molecules*; Oxford University Press: New York, 1989.

(2) (a) Versluis, L.; Ziegler, T. *J. Chem. Phys.* **1988**, *88*, 322. (b) Fan, L.; Versluis, L.; Ziegler, T.; Baerends, E. J.; Ravenek, W. *Int. J. Quantum Chem.* **1988**, *S22*, 173. (c) Harris, J.; Jones, R. O.; Muller, J. E. *J. Chem. Phys.* **1981**, *75*, 3904. (d) Fournier, R.; Andzelm, J.; Salahub, D. R. *J. Chem. Phys.* **1989**, *90*, 6371. (e) Delley, B.; *J. Chem. Phys.* **1991**, *94*, 7245. (f) Hohl, D.; Jones, R. O.; Car, R.; Parrinello, M. *J. Chem. Phys.* **1988**, *89*, 6823. (g) Jones, R. O.; Hohl, D. *J. Chem. Phys.* **1990**, *92*, 6710. (h) Mlynarsky, P.; Salahub, D. R. *J. Chem. Phys.* **1991**, *95*, 6050. (i) Fitzgerald, G.; Andzelm, J. *J. Phys. Chem.* **1991**, *95*, 10531. (l) Ziegler, T. *Chem. Rev.* **1991**, *91*, 651. (m) Fan, L.; Ziegler, T. *J. Am. Chem. Soc.* **1992**, *114*, 10890. (n) Bottoni, A. *J. Chem. Soc., Perkin Trans. 2* **1996,** 2041.

(3) (a) Hogeveen, H.; Volger, H. C. *J. Am. Chem. Soc.* **1967,** *89***,** 2486. (b) Katz, T. J.; Cerefice, S. A. *Ibid.* **1969**, *91*, 6519. (c) Cassar, L.; Eaton, P. E.; Halpern, J. *Ibid.* **1970,** *92***,** 3515. (d) Noyory, R.; Kumagai, Y.; Takaya, H. *Ibid.* **1974**, *96*, 634. (e) Binger, P.; Schroth, G.; McMeeking, J. *Angew. Chem., Int. Ed. Engl.* **1974**, *13*, 465. (f) Noyory, R.; Umeda, I.; Kawauchi, H.; Takaya, H. *Ibid.* **1975**, *97*, 812. (g) Doyle, M. J.; McMeeking, J.; Binger, P. *J. Chem. Soc., Chem. Commun.* **1976**, 376. (h) Mitsudo, T.; Kokuryo, K.; Shinsugi, T.; Nakagawa, Y.; Watanabe, Y.; Takegami, Y. *J. Org. Chem.* **1979**, *44*, 4492. (i) Mitsudo, T.; Hory, Y.; Watanabe, Y. *J. Organomet. Chem.* **1987**, *334*, 157. (l) Mitsudo, T.; Naruse, H.; Kondo, T.; Ozaki, Y. Watanabe, Y. *Angew. Chem., Int. Ed. Engl.* **1994,** *33***,** 580.

(4) (a) Huber, H.; Ozin, G. A.; Power, W. J. *J. Am. Chem. Soc.* **1976,** *98*, 6508. (b) Ozin, G. A.; Power, W. J.; Upton, T. H.; Goddard, W. A., III. *Ibid.* **1978**, *100*, 4750. (c) Merle-Mejean, T.; Cosse-Mertens, C.; Bouchareb, S.; Galan, F.; Mascetti, J.; Tranquille, M. *J. Phys. Chem.* **1992**, *96*, 9148. (d) Brown, C. E.; Mitchell, S. A.; Hackett, P. A. *Chem. Phys. Lett.* **1992,** *191*, 175. (e) Mitchell, S. A. *Int. J. Chem. Kinet.* **1994**, *26*, 97.

(5) (a) Rösch, N.; Hoffmann, R. *Inorg. Chem.* **1974**, *13*, 2656. (b) Akermark, B.; Almemark, M.; Almlöf, J.; Backwall, J. E.; Roos, B.; Stogard, A. J. *J. Am. Chem. Soc.* **1977**, *99*, 4617. (c) Upton, T. H.; Goddard, W. A., III. *J. Am. Chem. Soc.* **1978**, *100*, 321. (d) Basch, H.; Newton, M. D.; Moskowitz, J. W. *J. Chem. Phys.* **1978,** *69***,** 584. (e) Widmark, P.; Roos, B. O.; Siegbahn, P. E. M. *J. Phys. Chem.* **1985**, *89*, 2180. (f) Siegbahn, P. E. M.; Brandemark, U. B. *Theor. Chim. Acta* **1986**, *69*, 119. (g) Widmark, P.; Roos, B. O. *Ibid.* **1987**, *71*, 411. (h) Blomberg, R. A. M.; Siegbahn, P. E. M.; Lee, T. J.; Rendell, A. P.; Rice, J. E. *J. Chem. Phys.* **1991**, *95*, 5898. (i) Papai, I.; Fournier, R.; Salahub, D. R. *J. Phys. Chem.* **1993**, *97*, 9986. (l) Pierloot, K.; Persson, B. J.; Roos, B. O. *J. Phys. Chem.* **1995**, *99*, 3465.

(6) Andersson, K.; Blomberg, M. R. A.; Fülscher, M.; Kellö, V.; Lindh, R.; Malmqvist, P.-A.; Noga, J.; Olsen, J.; Roos, B. O.; Sadlej, A. J.; Siegbahn, P. E. M.; Urban, M.; Widmark, P.-O. *MOLCAS version 3*; University of Lund: Sweden, 1994.

(7) (a) Almlöf, J.; Taylor, P. R. *J. Chem. Phys.* **1987**, *86* 4070. (b) Bauschlicher, C. W., Jr.; Langhoff, S. R.; Kormornicki, A. *Theor. Chim. Acta* **1990**, *77*, 263.

(8) Dunning, T. H., Jr. *J. Chem. Phys.* **1989**, *90*, 1007.

(9) Basis sets were obtained from the Extensible Computational Chemistry Environment Basis Set Database, Version 1.0, as developed and distributed by the Molecular Science Computing Facility, Environmental and Molecular Sciences Laboratory, which is part of the Pacific Northwest Laboratory, P.O. Box 999, Richland, WA 99352, and funded by the U.S. Department of Energy. The Pacific Northwest Laboratory is a multiprogram laboratory operated by Battelle Memorial Institue for the U.S. Department of Energy under contract DE-AC06-76RLO 1830. Contact David Feller, Karen Schuchardt, or Don Jones for further information.

(10) Andersson, K.; Malmqvist, P.; Roos, B. O.; Sadlej, A. J.; Wolinski, K. *J. Phys. Chem.* **1990**, *94*, 5483. Andersson, K.; Malmqvist, P.; Roos, B. O. *J. Chem. Phys.* **1992**, *96*, 1218.

(11) Frisch, M. J.; Trucks, G. W.; Schlegel, H. B.; Gill, P. M. W.; Johnson, B. G.; Wong, M. W.; Foresman, J. B.; Robb, M. A.; Head-Gordon, M.; Replogle, E. S.; Gomperts, R.; Andres, J. L.; Raghavachari, K.; Binkley, J. S.; Gonzalez, C.; Martin, R. L.; Fox, D. J.; Defrees, D. J.; Baker, J.; Stewart, J. J. P.; Pople, J. A. *Gaussian 92/DFT*, Revision G.1; Gaussian, Inc.: Pittsburgh, PA, 1993.

(12) Godbout, N.; Salahub, D. R.; Andzelm, J.; Wimmer, E. *Can. J. Chem.* **1992**, *70*, 560.

(13) Hay, P. J.; Wadt, W. R. *J. Chem. Phys.* **1985**, *82*, 270. Hay, P. J.; Wadt, W. R. *J. Chem. Phys.* **1985**, *82* 284. Hay, P. J.; Wadt, W. R. *J. Chem. Phys.* **1985**, *82* , 299.

(14) (a) Hohenberg, P.; Kohn, W. *Phys. Rev. B* **1964**, *136*, 864. (b) Kohn, W.; Sham, L. J. *Phys. Rev. A* **1965**, *140*, 1133. (c) Becke, A. D. *Phys. Rev.* **1988**, *A38*, 3098. (d) Lee, C.; Yang, W.; Parr, R. G. *Phys. Rev.* **1988**, *B37*, 785. (e) Miehlich, A.; Savin, A.; Stoll, H.; Preuss, H. *Chem. Phys. Lett.* **1989**, *157*, 200. (f) Perdew, J. P.; Zunger, A. *Phys. Rev.* **1981**, *B23*, 5048. (g) Perdew, J. P. *Phys. Rev.* **1986**, *B33*, 8822. (h) Becke, A. D. *Int. J. Quantum Chem.* **1989**, *S23*, 599. (i) Becke, A. D. *J. Chem. Phys.* **1993**, *98*, 5648.